CHAPTER VI
PREPARATION OF SOL-GEL/PURIFIED SODIUM-BENTONITE COMPOSITES AND THEIR PHOTOVOLTAIC APPICATION FOR DYE-SENSITIZED SOLAR CELLS

6.1 Abstract

The sol-gel TiO_2/purified natural clay electrodes having Ti:Si molar ratios of 95:5 and 90:10 were initially prepared, sensitized with natural red cabbage dye, and compared to the sol-gel TiO_2 electrode in terms of physicochemical characteristics and solar cell efficiency. The results showed that the increase in purified Na-bentonite content greatly increased the specific surface area and total pore volume of the prepared sol-gel TiO_2/purified Na-bentonite composites because the clay platelets prevented TiO_2 particle agglomeration. The sol-gel TiO_2/5 mol% Si purified Na-bentonite and sol-gel TiO_2/10 mol% Si purified Na-bentonite composites could increase the film thickness without cracking when they were coated as a scattering layer on the TiO_2 semiconductor-based film, leading to increasing the efficiency of the natural dye-sensitized solar cells in this work.

Keywords: Sol-gel TiO_2; Purified natural clay; Dye-sensitized solar cell; Red cabbage dye; Scattering layer

6.2 Introduction

Dye-sensitized solar cell (DSSC) was firstly developed by Grätzel's group [1-3] and has widely known as a low-cost and easy-assembly solar cell. However, many synthetic dyes normally used as the electron generator, a main component in the DSSC, are very expensive as compared to another DSSC component, which is widely used. TiO_2 semiconductor acting as both the host for adsorption of dye molecules and the electron transport pathway. A way to lower the cost of DSSC is to reduce the amount of expensive synthetic dyes by employing thinner sensitized

films. Nevertheless, this would decrease the amount of light absorbed by the dye molecules. Light scattering phenomenon can help effectively increase light absorption path length, especially in thinner films, in which charge recombination can be reduced due to a lower film resistance [4,5]. Large TiO_2 particle with size of about 70-1,000 nm and other different refractive index materials can be used as light scattering centers by admixing with smaller TiO_2 particles with size of about 10-25 nm [5-7]. Besides, some other inactive particles [5] or flakes [8] have also been used as scattering layers or reflectors on the back side of photoelectrodes.

Interestingly, Park et al. [9] applied synthetic clay nanoparticles in order to solidify liquid electrolyte and induce light scattering in the DSSCs, which helped increase the overall light absorption, especially in the red region. With 500-2,000 nm platelet size, the abundant natural Na-bentonite clay, with a chemical formula of $(Na,Ca)_{0.33}(Al,Mg)_2(Si_4O_{10})(OH)_2 \cdot nH_2O$ [10], is also believed to be able to function as the light scattering site in the DSSCs. Not only can light scattering effect be employed for DSSCs sensitized with synthetic dyes, but it can be also employed to increase light absorption ability of natural dyes. Because of low material cost, simple preparation, and lack of heavy metals, natural dyes are more favorable to be applied for such environmentally friendly device [11-14]. Particularly, the dye extracted from red cabbage has been proven to provide comparatively high DSSC efficiency among various natural dyes [14-15].

In this present work, the sol-gel TiO_2/purified natural Na-bentonite clay composite having Ti:Si molar ratios of 95:5 and 90:10 were therefore prepared. They were, for the first time, applied for the DSSCs sensitized with the natural red cabbage dye, as compared to the sol-gel TiO_2 electrode in terms of physicochemical characteristics and solar cell efficiency to verify the potential application of natural clay for the DSSCs.

6.3 Experimental Details

6.3.1 Preparation of Red Cabbage Dye Sensitizer

Fresh red cabbage was cut into very small pieces and then extracted in a methanol/water (3:1 by volume) mixed solvent. Afterward, the solid residues were

filtered out. Then, the dye solution was concentrated by a rotary evaporator at 50°C and finally stored at 4°C before use.

6.3.2 Na-Bentonite Clay Purification

Reverse osmosis (RO) water with 30 times by weight was used to swell raw Na-bentonite under vigorous stirring for 12 h. The swollen Na-bentonite was centrifuged at 10,000 rpm for 10 min. Then, the supernatant containing highly dispersed swollen Na-bentonite, which had the main compositions of 78.5 wt.% SiO_2, 16.4 wt.% Al_2O_3, 2.4 wt.% Fe_2O_3, and 1.7 wt.% MgO obtained from X-ray fluorescence analysis, was collected, dried, and ground in mortar.

6.3.3 Preparation of Photoanodes

TiO_2 sol was prepared by hydrolyzing diisopropoxytitanate bis(acetylacetonate) with water at a molar ratio of 1:30. The solution was heated to 70°C until it became transparent. Next, polyethylene glycol (MW of 20,000) was added to the TiO_2 sol with the TiO_2-to-polyethylene glycol weight ratio of 3.3:1. The purified Na-bentonite was swollen in RO water with 40 times by weight for 12 h before mixing with the TiO_2 sol at 50°C for 6 h. The Ti:Si molar ratio of the TiO_2/purified Na-bentonite composite were controlled at 95:5 and 90:10. Then, the gel was formed at 80°C. Afterwards, the gel-derived paste was smoothly spread on fluorine-doped SnO_2 (FTO) glasses (sheet resistance of 15 Ω/cm^2) by the doctor blading method and calcined at 500°C for 1 h to obtain the photoanode film. Then, the calcined film was immersed into the extracted red cabbage dye solution.

6.3.4 Cell Assembly

To assemble the DSSCs cell, the 80 μm-thick transparent sticker film was used to make a narrow empty space inside the cell, by attaching around the four edges between the as-prepared semiconductor photoanode film and the Pt cathode film prepared from 7 mM hexachloroplatinic acid in 2-propanol by using the spin-coating technique. The electrolyte consisting of 0.1 M LiI, 0.05 M I_2, and 0.4 M 4-

tert-butylpiridine in acetonitrile was dropped and injected to spread thoroughly in the as-prepared space between the two electrodes.

6.3.5 Characterization and Measurement

The photoanodes were characterized by using an X-ray diffractometer (XRD, Bruker Model-D8 Advance), a scanning electron microscope (SEM, Hitachi S4800), a transmission electron microscope (TEM, JEOL JEM-2100), and a N_2 adsorption-desorption analyzer (Autosorb-1, Quantachrome). The photovoltaic properties of the prepared DSSCs, i.e. short circuit current (J_{sc}, mA/cm^2), open circuit voltage (V_{oc}, V), fill factor (FF), and efficiency (ŋ, %), were determined from the I–V curve obtained by using a digital Keithley 236 multimeter under an irradiation of white light from a 1000 W/HS Xenon arc lamp with a 100 mW/cm^2 light intensity, where the fill factor and efficiency were calculated based on the following equations:

$$FF = \frac{J_{max} \times V_{max}}{J_{sc} \times V_{oc}} \quad (6.1)$$

$$\eta = \frac{J_{sc} \times V_{oc} \times FF}{P_{in}} \quad (6.2)$$

where J_{max} is maximum power point current (mA/cm^2), V_{max} is maximum power point voltage (V), and P_{in} is power of incident light (mW/cm^2).

6.4 Results and Discussion

6.4.1 Characterization Results of Prepared Semiconductors

Fig.6.1 shows XRD patterns of the pure sol-gel TiO_2 and sol-gel TiO_2/purified Na-bentonite composites which the anatase TiO_2 phase was mainly detected. The presence of the bentonite phase was clearly observed in both sol-gel TiO_2/5 mol% Si purified Na-bentonite and sol-gel TiO_2/10 mol% Si purified Na-bentonite composites at diffraction angles of approximately 6°. The particle size of the prepared sol-gel TiO_2 from both the SEM and TEM analysis was about 5-10 nm,

as shown in Fig. 6.2. The textural properties from the N_2 adsorption-desorption analysis shown in Table 6.1 revealed that an increase in purified Na-bentonite content significantly increased the specific surface area and total pore volume of the prepared TiO_2/purified Na-bentonite composites, while the mean pore size became almost unchanged. These may be because the TiO_2 nanoparticles were inserted between the clay platelets in the composite-made electrode, thus preventing their tight agglomeration, as shown by the cross-sectional SEM micrographs in Fig. 6.3. It can also be observed from Fig. 6.3b that the clay platelets were highly distributed in the sol-gel TiO_2/purified Na-bentonite electrode. In addition, from direct observation during the electrode preparation, the increase in purified Na-bentonite content increased the ability to increase the film thickness without cracking.

6.4.2 Photovoltaic Properties of Different Photoanodes

As shown in Table 6.2, at low thickness of about 1 μm, the sol-gel TiO_2/5 mol% Si purified Na-bentonite electrode exhibited the efficiency and other photovoltaic properties nearly the same as those of the pure sol-gel TiO_2 electrode due to a low resistivity of the film with low clay content. However, as observed in Fig. 6.3b, the most preferentially orientated direction of clay platelets in the electrode was in the horizontal plane. Therefore, the clay platelets can retard the flow of ions in electrolyte and also resist the flow of current through the electrode. Thus, too much addition of purified Na-bentonite reduced the short circuit current and fill factor [16]. This was also experimentally observed in this present work that at the same thickness of about 3.5 μm, the sol-gel TiO_2/10 mol% Si purified Na-bentonite electrode gave a lower efficiency than the electrode with the sol-gel TiO_2/5 mol% Si purified Na-bentonite (Table 6.2). Moreover, the sol-gel TiO_2/5 mol% Si purified Na-bentonite could be used to increase the film thickness without cracking when it was coated as a scattering layer on the TiO_2 semiconductor-based film. This led to an increase in the efficiency of the cells, as shown in Table 6.3. The same results were also observed when using the sol-gel TiO_2/10 mol% Si purified Na-bentonite as a scattering layer, but with less improvement of the cell performances than the sol-gel TiO_2/5 mol% Si purified Na-bentonite. Therefore, the purified Na-bentonite with 5 mol% Si was

considered to be the optimum clay content. A possible reason for the improvement of the cell performances might be the increase in light harvesting ability of the electrode due to the multiple light scattering in the film in the presence of the clay as light scattering sites. In addition, the increased amount of adsorbed dye in the film due to the increased thickness was another possible reason, as experimentally observed.

6.5 Conclusions

The sol-gel TiO_2/5 mol% Si purified Na-bentonite and sol-gel TiO_2/10 mol% Si purified Na-bentonite composites were prepared and applied for the DSSCs electrodes sensitized with red cabbage dye. They could increase the film thickness without cracking when coated as a scattering layer on the TiO_2 semiconductor-based film, which helped increase the cell performances. The optimum clay content was found to be 5 mol% Si purified Na-bentonite.

6.6 Acknowledgments

This work was financially supported by the Royal Golden Jubilee Ph.D. Program, Thailand; Rachadapiseksompote Endowment, Chulalongkorn University, Thailand; and National Nanotechnology Center, National Science and Technology Development Agency, Thailand. The authors also would like to thank Thai Nippon Chemical Industry Co., Ltd for kindly providing the clay.

6.7 References

[1] Nazeeruddin MK, Kay A, Rodicio I, Humphry-Baker R, Müller E, Liska P, et al. Conversion of Light to Electricity by Cis-X_2bis(2,2′-Bipyridyl-4,4′-Dicarboxylate)Ruthenium(II) Charge-Transfer Sensitizers (X = Cl-, Br-, I-, CN-, and SCN-) on Nanocrystalline TiO_2 Electrodes. J. Am. Chem. Soc. 1993; 115: 6382-90.

[2] Barbé CJ, Arendse F, Comte P, Jirousek M, Lenzmanne F, Shklover V, et al. Nanocrystalline Titanium Oxide Electrodes for Photovoltaic Applications. J. Am. Ceram. Soc. 1997; 80: 3157-71.

[3] Kalyanasundaram K, Grätzel M. Coord. Applications of Functionalized Transition Metal Complexes in Photonic and Optoelectronic Devices. Chem. Rev. 1998; 177: 347-414.

[4] Usami A. Theoretical Simulations of Optical Confinement in Dye-Sensitized Nanocrystalline Solar Cells. Sol. Energy Mater. Sol. Cells 2000; 64: 73-83.

[5] Hore S, Vetter C, Kern R, Smit H, Hinsch A. Influence of Scattering Layers on Efficiency of Dye-Sensitized Solar Cells. Sol. Energy Mater. Sol. Cells 2006; 90: 1176-88.

[6] Wang ZS, Kawauchi H, Kashima T, Arakawa H. Significant Influence of TiO_2 Photoelectrode Morphology on the Energy Conversion Efficiency of N719 Dye-Sensitized Solar Cell. Coord. Chem. Rev. 2004; 248: 1381-89.

[7] Ferber J, Luther J. Computer Simulation of Light Scattering and Absorption in Dye-Sensitized Solar Cells. Sol. Energy Mater. Sol. Cells 1998; 54: 265-75.

[8] Yasuda T, Ikeda S, Furukawa S. Synthesis of Reflective TiO_2/SiO_2 Multilayer Flakes for Solar cell Application. Dyes. Pigments. 2010; 86: 278-81.

[9] Park JH, Kim BW, Moon JH. Dual Functions of Clay Nanoparticles with High Aspect Ratio in Dye-Sensitized Solar Cells. Electrochem. Solid-State Lett. 2008; 11: B171-3.

[10] Plummer CC, McGeary D, Carlson DH. Physical Geology. 8th ed. Boston :WCB McGraw-Hill; 1999.

[11] Garcia CG, Polo AS, Iha NYM. Fruit Extracts and Ruthenium Polypyridinic Dyes for Sensitization of TiO_2 in Photoelectrochemical Solar Cells. J. Photochem. Photobiol. A: Chem. 2003; 160: 87-91.

[12] Hao S, Wu J, Huang Y, Lin J. Natural Dyes as Photosensitizers for Dye-Sensitized Solar Cell. Sol. Energy 2006; 80: 209-14.

[13] Polo AS, Iha NYM. Blue Sensitizers for Solar Cells: Natural Dyes from Calafate and Jaboticaba. Sol. Energy Mater. Sol. Cells 2006; 90: 1936-44.

[14] Calogero G, Marco GD. Red Sicilian Orange and Purple Eggplant Fruits as Natural Sensitizers for Dye-Sensitized Solar Cells. Sol. Energy Mater. Sol. Cells 2008 ; 92: 1341-6.

[15] Furukawa S, Iino H, Iwamoto T, Kukita K, Yamauchi S. Characteristics of Dye-Sensitized Solar Cells Using Natural Dye, Thin Solid Films 2009; 518: 526-9.

[16] Hugfeldt A, Didriksson B, Palmqyist T, Lindström H, Södergren S, Rensmo H, et al. Verification of High Efficiencies for the Grätzel–cell. A 7% Efficient Solar Cell Based on Dye-Sensitized Colliodal TiO_2. Sol. Energy Mater. Sol. Cells 1994; 31: 481-8.

Table 6.1 Textural properties of the semiconductor electrodes obtained from N_2 adsorption-desorption analysis

Semiconductor electrode	Specific surface area (m^2/g)	Mean pore size (nm)	Total pore volume (cm^3/g)
Sol-gel TiO_2	120	3.61	0.163
Sol-gel TiO_2/5 mol% Si purified Na-bentonite	165	3.63	0.215
Sol-gel TiO_2/10 mol% Si purified Na-bentonite	198	3.64	0.246
Purified Na-bentonite	62	-	-

Table 6.2 Photovoltaic properties of DSSCs sensitized by red cabbage dye

Semiconductor electrode	Thickness (μm)	J_{sc} (mA/cm^2)	V_{oc} (V)	FF	η (%)
TiO_2	~0.9	0.60	0.59	0.28	0.10
Sol-gel TiO_2/5 mol% Si purified Na-bentonite	~1.5	0.59	0.59	0.27	0.09
	~3.5	0.80	0.58	0.23	0.11
Sol-gel TiO_2/10 mol% Si purified Na-bentonite	~3.5	0.08	0.49	0.90	0.04

Table 6.3 Photovoltaic properties of DSSCs fabricated with light scattering layer and sensitized by red cabbage dye

Semiconductor electrode	Scattering layer	TiO_2/total thickness (μm)	J_{sc} (mA/cm^2)	V_{oc} (V)	FF	η (%)
TiO_2	Sol-gel TiO_2/5 mol% Si purified Na-bentonite	~0.8/1.4	0.89	0.60	0.32	0.17
	Sol-gel TiO_2/10 mol% Si purified Na-bentonite	~0.8/1.6	0.68	0.58	0.36	0.14

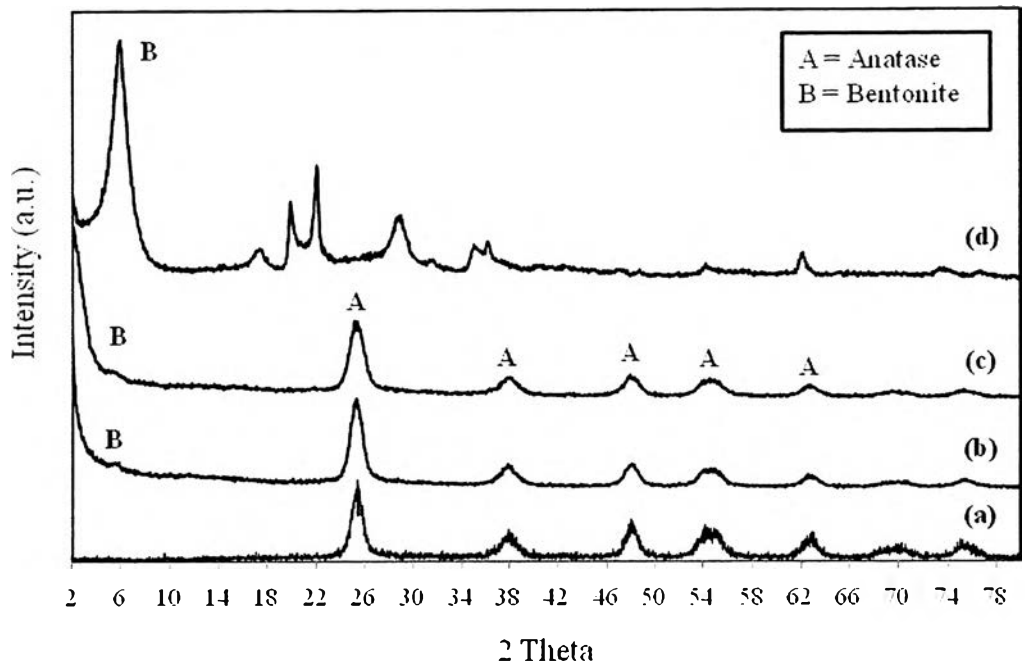

Figure 6.1 XRD patterns of (a) sol-gel TiO_2, (b) sol-gel TiO_2/5 mol% Si purified Na-bentonite, (c) sol-gel TiO_2/10 mol% Si purified Na-bentonite electrodes and (d) purified Na-bentonite.

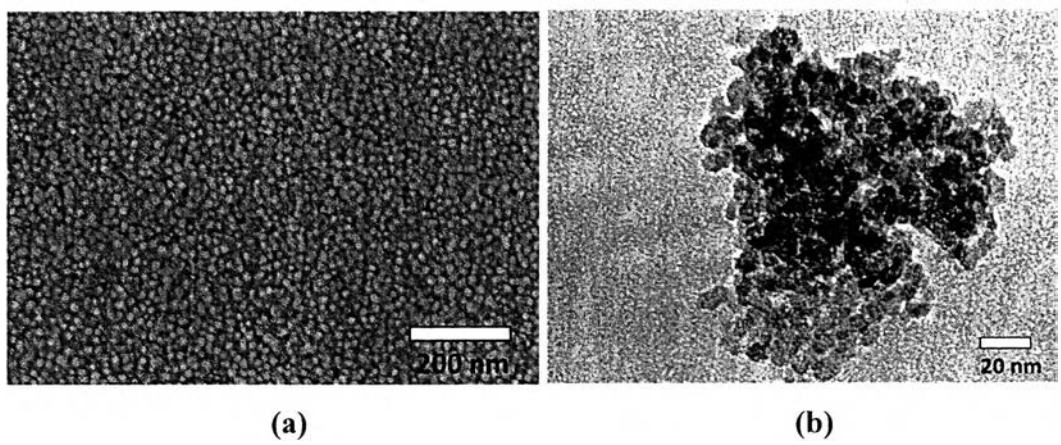

Figure 6.2 SEM micrograph (a) and TEM micrograph (b) of sol-gel TiO_2.

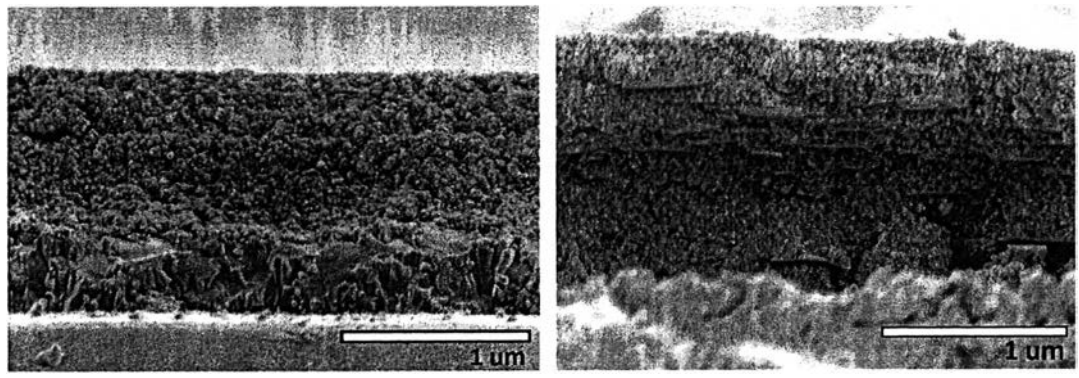

(a) **(b)**

Figure 6.3 Cross-sectional SEM micrographs of (a) sol-gel TiO_2 and (b) sol-gel TiO_2/5 mol% Si purified Na-bentonite electrodes.